Simulation of the influence of N_2O on the chemical stage of water radiolysis

JIŘÍ BARILLA, PAVEL SIMR, KVĚTUŠE SÝKOROVÁ

Faculty of Science, Department of Informatics,
J. E. Purkyne University in Usti nad Labem
Pasteurova 3544/1, 400 96 Usti nad Labem
CZECH REPUBLIC

Abstract: - The absorption of ionizing radiation causes the radiolysis of water to form aggressive radicals. Water radiolysis plays an essential role in radiotherapy, radio sterilization, food irradiation, and wastewater irradiation because living cells consist mainly of water. Radical clusters arise immediately after irradiating water with ionizing radiation, and aggressive radicals damage living cells. These damages are caused mainly by SSB and DSB formation on DNA molecules. The mathematical simulation model, created with the help of Continuous Petri nets, is very suitable to study the dynamics of the chemical stage of water radiolysis. This mathematical simulation model, which includes the influence of oxygen on the chemical stage of radiobiological mechanism, was created in our previous work. This paper is extended to include the influence of N2O. The presence of N2O during irradiation of water plays a vital role because it increases OH radicals, which are mainly responsible for DNA damage. The mathematical model enables us to simulate the dynamics of the chemical reactions and the diffusion of radical clusters during chemical stage of water radiolysis.

Key-Words: - Continuous Petri nets, water radiolysis, the influence of N_2O, radical clusters, simulation model

Received: April 14, 2021. Revised: January 23, 2022. Accepted: February 24, 2022. Published: April 2, 2022.

1 Introduction

The radiolysis of water is caused by the absorption of ionizing radiation in water medium to form aggressive radicals $H^{\bullet}, OH^{\bullet}$ and $HO_2^{\bullet}$, hydrated electrons e_{aq}^{-}, and H_3O^{+} ions. These radicals diffuse into surroundings and can damage the DNA molecule if their concentration is sufficient when they meet the DNA. Mainly OH radicals are responsible for the formation of SSB (Single-Strand Breaks) and DSB (Double-Strand Breaks) on DNA molecules. The damages of DNA molecules caused by aggressive radicals run mainly through indirect effects when energy is absorbed outside the DNA molecule. The indirect effect occurs when using low-LET radiation.
After the energy is transferred to the water, a radical cluster is formed, and radicals inside the cluster diffuse into surroundings and react mutually and with other molecules present in water. The concentration of radicals and, therefore, their radiobiological effect is influenced by the presence of other substances which can have radioprotective or radiosensitive character. Radioprotective and radiosensitive substances are used mainly in radiotherapy to protect healthy cells against ionizing radiation or sensitize cancer cells to obtain a greater radiobiological effect.
To study the dynamics of the chemical stage of water radiolysis, the mathematical models created with the help of Continuous Petri nets are very suitable. The main reason is that Petri nets allow us to solve easily complicated systems such as chemical reactions of the radicals, ions, and other products of water radiolysis together with diffusion of the radical clusters which run simultaneously. Petri nets enable us to use graphical tools to create mathematical models, taking much less time than classical programming. Also, the testing and the changes are faster, too.
At the beginning of our research, we used the programming language to create the mathematical models describing the chemical stage of water radiolysis [3][5]. Then, to quickly solve more detailed and complicated mathematical models, we further used the Continuous Petri nets in the research [4][6][7][8][9]. We compared these simulated mathematical models with the experimental data and achieved good consent.

The tested mathematical model has been used to describe the influence of oxygen on the chemical stage of the radiobiological mechanism in a paper [8]. The indirect effect of the radiobiological mechanism is caused by aggressive radicals formed during the radiolysis of water. The influence of oxygen on the chemical stage of the radiobiological mechanism plays an important role mainly in radiotherapy because the oxygen concentration is higher in healthy cells than in cancer cells. Therefore, radiation sensitivity is different for healthy cells and cancer cells. The dependence of the concentrations of individual radicals on time under various oxygen concentrations is showed to explain the oxygen effect. The obtained results were compared with experimental data, and a good agreement was achieved.

In this paper, the influence of N2O on the chemical stage of water radiolysis was analyzed with the help of Continuous Petri nets. The time dependencies of the concentrations of individual radicals under various N2O concentrations were simulated to show the impact of N2O molecules on radical concentrations, mainly increasing concentration of OH radicals, which results in more significant damage to the DNA molecule. To create our mathematical model, using Continuous Petri nets, primary products of water radiolysis ($e_{aq}^{-}, H^{\bullet}, OH^{\bullet}, H_3O^{+}$), and associated products (OH^{-}, H_2, H_2O_2, O_2^{-}, $HO_2^{\bullet}$, O_2) were taken into account. Their initial yields and physicochemical constants have been taken from the literature dealing with the radiolysis of water, for example [10][12][13][14][18][19][20][21][26][27]. As in previous publications, the corresponding radical clusters (at low-LET radiation) were described as spherically symmetric systems [21].

2 Mathematical model of the influence of N2O on the chemical stage of water radiolysis

The basic mathematical model of the chemical stage of water radiolysis was created in our previous papers [6][7][8]. The mathematical model in this paper is extended to include the influence of N2O on the chemical stage of water radiolysis. Therefore, we will not repeat the derivation of the mathematical model, and only the short overview will be done.

The basic assumptions of the mathematical model are:

- Water radicals arise inside the diffusing radical cluster, containing a nonhomogeneous concentration of individual species [22].
- Individual radicals diffuse differently, according to their diffusion coefficients, must also be included in the mathematical model. Diffusion coefficients are taken from the literature.
- Immediately after cluster formation, simultaneously with the diffusion of radicals also the chemical reactions of radicals and other species present in the cluster run. Their rate constants are taken from the literature, too.
- In our mathematical model, we assume a spherical symmetry of the diffusion clusters [22], and initial conditions are given by the volume $V_i(t = 0) = V_0$ of the cluster and by the numbers of corresponding radicals $N_i(t = 0)$.

All these conditions are described in detail in our previous papers, where the general mathematical model has been derived, too. In this paper, only the final mathematical model, simulating the influence of N2O, will be presented. The dynamics of the cluster evolution can be described by a system of ordinary differential equations, which solve the diffusion of radicals and their chemical reactions.

To solve the system of ordinary differential equations, the Continuous Petri nets have been used. Petri nets enable us to easily create the mathematical model with the help of graphical tools as well as to perform the rapid simulations, which allows us to optimize the parameters of the simulation model [16][17][24][25]. The detailed description of the solution of our mathematical model using Petri nets can be found in [6][7][8], where Petri nets are also sufficiently described.

The radicals, ions, and other substances arising inside the cluster, and diffuse into the surroundings, are presented in Table I, where we can also see their diffusion coefficients and designation. All diffusion coefficients are taken from the literature. We will assume that at the beginning of the cluster diffusion (at time t0), when the chemical reactions start, only the following species will be present: $H^{\bullet}$, $OH^{\bullet}$, e_{aq}^{-}, H_3O^{+} and H_2. In Table II, we can see chemical reactions running after cluster formation, which is considered in our mathematical model. The rate constants of the chemical reactions presented in Table II are also taken from the literature.

Table 1. Diffusion coefficients [19]

Substance		Diffusion coefficient ($nm^2.ns^{-1}$)	Species amount	Designation of diff. coefficients
1.	$H^\bullet$	7.0	N_H	D_H
2.	$OH^\bullet$	2.2	N_{OH}	D_{OH}
3.	e_{aq}^-	4.9	N_e	D_e
4.	H_3O^+	9.5	$N_{H_3O^+}$	$D_{H_3O^+}$
5.	OH^-	5.3	N_{OH^-}	D_{OH^-}
6.	H_2	5	N_{H_2}	D_{H_2}
7.	H_2O_2	2.2	$N_{H_2O_2}$	$D_{H_2O_2}$
8.	O_2^-	1.8	$N_{O_2^-}$	$D_{O_2^-}$
9.	$HO_2^\bullet$	2.3	N_{HO_2}	D_{HO_2}

Table 2. Recombination reactions [14]

Reaction			Rate constants ($dm^3.mole^{-1}.s^{-1}$)
1.	$H^\bullet + H^\bullet \rightarrow$	H_2	10×10^{10}
2.	$e_{aq}^- + H^\bullet \rightarrow$	$H_2 + OH^-$	2.5×10^{10}
3.	$e_{aq}^- + e_{aq}^- \rightarrow$	$H_2 + 2OH^-$	6×10^9
4.	$e_{aq}^- + OH^\bullet \rightarrow$	$OH^- + H_2O$	3×10^{10}
5.	$H^\bullet + OH^\bullet \rightarrow$	H_2O	2.4×10^{10}
6.	$OH^\bullet + OH^\bullet \rightarrow$	H_2O_2	4×10^9
7.	$H_3O^+ + e_{aq}^- \rightarrow$	$H^\bullet + H_2O$	2.3×10^{10}
8.	$HO_2^\bullet + H^\bullet \rightarrow$	H_2O_2	1×10^{10}
9.	$HO_2^\bullet + OH^\bullet \rightarrow$	$H_2O + O_2$	1×10^{10}
10.	$HO_2^\bullet + HO_2^\bullet \rightarrow$	$H_2O_2 + O_2$	2×10^6
11.	$O_2^- + H_3O^+ \rightarrow$	$HO_2^\bullet$	3×10^{10}
12.	$H_3O^+ + OH^- \rightarrow$	H_2O	1×10^{11}
13.	$H^\bullet + H_2O_2 \rightarrow$	$H_2O + OH^\bullet$	1×10^8
14.	$e_{aq}^- + H_2O_2 \rightarrow$	$OH^\bullet + OH^-$	1.2×10^{10}
15.	$OH^\bullet + H_2O_2 \rightarrow$	$H_2O + HO_2^\bullet$	5×10^7
16.	$OH^\bullet + H_2 \rightarrow$	$H_2O + H^\bullet$	6×10^7
17.	$HO_2^\bullet \rightarrow$	$H_3O^+ + O_2^-$	1×10^6
18.	$e_{aq}^- + O_2 \rightarrow$	$O_2^- + H_2O$	1.9×10^{10}
19.	$H^\bullet + O_2 \rightarrow$	$HO_2^\bullet$	1×10^{10}
20.	$e_{aq}^- + N_2O \rightarrow$	$N_2 + OH^- + OH^\bullet$	9.1×10^9

Compared to our previous works, mainly [8], the chemical reaction 20 (see Table II) has been added. This chemical reaction expresses the influence of N_2O on the chemical stage of water radiolysis, such that the number of OH radicals is increased, which results in more significant damage to the DNA molecule.

Using the diffusion coefficients from Table I and the chemical reactions from Table II, we can describe the whole dynamics process of the chemical stage of water radiolysis, where spherical symmetry of the cluster evolution is assumed, by the following system of ordinary differential equations:

$$\frac{dN_H}{dt} = -2k_1\frac{N_H(t)N_H(t)}{V_H(t)} - k_2\frac{N_H(t)N_e(t)}{V_H(t)} - k_5\frac{N_H(t)N_{OH}(t)}{V_H(t)} - k_8\frac{N_H(t)N_{HO_2}(t)}{V_H(t)} - k_{13}\frac{N_H(t)N_{H_2O_2}(t)}{V_H(t)} - k_{19}\frac{N_H(t)N_{O_2}(t)}{V_H(t)} + k_7\frac{N_e(t)N_{H_3O^+}(t)}{V_{H_3O^+}(t)} + k_{16}\frac{N_{OH}(t)N_{H_2}(t)}{V_{H_2}(t)} \quad (1)$$

$$\frac{dN_{OH}}{dt} = -k_4\frac{N_{OH}(t)N_e(t)}{V_e(t)} - k_5\frac{N_{OH}(t)N_H(t)}{V_H(t)} - 2k_6\frac{N_{OH}(t)N_{OH}(t)}{V_{OH}(t)} - k_9\frac{N_{OH}(t)N_{HO_2}(t)}{V_{HO_2}(t)} - k_{15}\frac{N_{OH}(t)N_{H_2O_2}(t)}{V_{OH}(t)} - k_{16}\frac{N_{OH}(t)N_{H_2}(t)}{V_{H_2}(t)} + k_{13}\frac{N_H(t)N_{H_2O_2}(t)}{V_H(t)} + k_{14}\frac{N_e(t)N_{H_2O_2}(t)}{V_e(t)} + k_{20}\frac{N_e(t)N_{N_2O}(t)}{V_e(t)} \quad (2)$$

$$\frac{dN_e}{dt} = -k_2\frac{N_H(t)N_e(t)}{V_H(t)} - 2k_3\frac{N_e(t)N_e(t)}{V_e(t)} - k_4\frac{N_{OH}(t)N_e(t)}{V_e(t)} - k_7\frac{N_e(t)N_{H_3O^+}(t)}{V_{H_3O^+}(t)} - k_{14}\frac{N_e(t)N_{H_2O_2}(t)}{V_e(t)} - k_{18}\frac{N_e(t)N_{O_2}(t)}{V_e(t)} - k_{20}\frac{N_e(t)N_{N_2O}(t)}{V_e(t)} \quad (3)$$

$$\frac{dN_{H_3O^+}}{dt} = -k_7\frac{N_e(t)N_{H_3O^+}(t)}{V_{H_3O^+}(t)} - k_{11}\frac{N_{H_3O^+}(t)N_{O_2^-}(t)}{V_{H_3O^+}(t)} - k_{12}\frac{N_{H_3O^+}(t)N_{OH^-}(t)}{V_{H_3O^+}(t)} + k_{17}N_{(HO_2)}(t) \quad (4)$$

$$\frac{dN_{OH^-}}{dt} = -k_{12}\frac{N_{H_3O^+}(t)N_{OH^-}(t)}{V_{H_3O^+}(t)} + k_2\frac{N_H(t)N_e(t)}{V_H(t)} + 2k_3\frac{N_e(t)N_e(t)}{V_e(t)} + k_4\frac{N_{OH}(t)N_e(t)}{V_e(t)} + k_{14}\frac{N_e(t)N_{H_2O_2}(t)}{V_e(t)} + k_{20}\frac{N_e(t)N_{N_2O}(t)}{V_e(t)} \quad (5)$$

$$\frac{dN_{H_2}}{dt} = -k_{16}\frac{N_{OH}(t)N_{H_2}(t)}{V_{H_2}(t)} + k_1\frac{N_H(t)N_H(t)}{V_H(t)} + k_2\frac{N_H(t)N_e(t)}{V_H(t)} + k_3\frac{N_e(t)N_e(t)}{V_e(t)} \quad (6)$$

$$\frac{dN_{H_2O_2}}{dt} = -k_{13}\frac{N_H(t)N_{H_2O_2}(t)}{V_H(t)} - k_{14}\frac{N_e(t)N_{H_2O_2}(t)}{V_e(t)} - k_{15}\frac{N_{OH}(t)N_{H_2O_2}(t)}{V_{OH}(t)} + k_6\frac{N_{OH}(t)N_{OH}(t)}{V_{OH}(t)} + k_8\frac{N_H(t)N_{HO_2}(t)}{V_H(t)} + k_{10}\frac{N_{HO_2}(t)N_{HO_2}(t)}{V_{HO_2}(t)} \quad (7)$$

$$\frac{dN_{O_2^-}}{dt} = -k_{11}\frac{N_{H_3O^+}(t)N_{O_2^-}(t)}{V_{H_3O^+}(t)} + k_{17}N_{HO_2}(t) + k_{18}\frac{N_e(t)N_{O_2}(t)}{V_e(t)} \quad (8)$$

$$\frac{dN_{HO_2}}{dt} = -k_8\frac{N_H(t)N_{HO_2}(t)}{V_H(t)} - k_9\frac{N_{OH}(t)N_{HO_2}(t)}{V_{HO_2}(t)} - 2k_{10}\frac{N_{HO_2}(t)N_{HO_2}(t)}{V_{HO_2}(t)} - k_{17}N_{HO_2}(t) + k_{11}\frac{N_{H_3O^+}(t)N_{O_2^-}(t)}{V_{H_3O^+}(t)} + k_{15}\frac{N_{OH}(t)N_{H_2O_2}(t)}{V_{OH}(t)} + k_{19}\frac{N_H(t)N_{O_2}(t)}{V_H(t)} \quad (9)$$

$$\frac{dN_{O_2}}{dt} = -k_{18}\frac{N_e(t)N_{O_2}(t)}{V_e(t)} - k_{19}\frac{N_H(t)N_{O_2}(t)}{V_H(t)} + k_9\frac{N_{OH}(t)N_{HO_2}(t)}{V_{HO_2}(t)} + k_{10}\frac{N_{HO_2}(t)N_{HO_2}(t)}{V_{HO_2}(t)} \quad (10)$$

$$\frac{dN_{N_2O}}{dt} = -k_{20}\frac{N_e(t)N_{N_2O}(t)}{V_e(t)} \quad (11)$$

where N_H, N_{OH}, N_e, $N_{H_3O^+}$, N_{OH^-}, N_{H_2}, $N_{H_2O_2}$, $N_{O_2^-}$, N_{HO_2}, N_{O_2} and N_{N_2O} represent numbers of species H, OH, e, H_3O^+, OH^-, H_2, H_2O_2, O_2^-, HO_2, O_2 and N_2O, which are placed in corresponding volumes V_H, V_{OH}, V_e, $V_{H_3O^+}$, V_{OH^-}, V_{H_2}, $V_{H_2O_2}$, $V_{O_2^-}$ and V_{HO_2}. k_1, k_2, ..., k_{20} are rate constants of the chemical reactions from Table II.

Immediately after cluster formation, radicals diffuse into surroundings and volumes V_H, V_{OH}, V_e, $V_{H_3O^+}$, V_{OH^-}, V_{H_2}, $V_{H_2O_2}$, $V_{O_2^-}$ and V_{HO_2} are increased according to the system of ordinary differential equations: $\frac{dV_H}{dt} = 128\sqrt{\left(\frac{D_H^3 t}{\pi}\right)}$,

$$\frac{dV_{OH}}{dt} = 128\sqrt{\left(\frac{D_{OH}^3 t}{\pi}\right)}, \quad (13)$$

(12)

$$\frac{dV_e}{dt} = 128\sqrt{\left(\frac{D_e^3 t}{\pi}\right)}, \quad (14)$$

$$\frac{dV_{H_3O^+}}{dt} = 128\sqrt{\left(\frac{D_{H_3O^+}^3 t}{\pi}\right)}, \quad (15)$$

$$\frac{dV_{OH^-}}{dt} = 128\sqrt{\left(\frac{D_{OH^-}^3 t}{\pi}\right)}, \quad (16)$$

$$\frac{dV_{H_2}}{dt} = 128\sqrt{\left(\frac{D_{H_2}^3 t}{\pi}\right)}, \quad (17)$$

$$\frac{dV_{H_2O_2}}{dt} = 128\sqrt{\left(\frac{D_{H_2O_2}^3 t}{\pi}\right)}, \quad (18)$$

$$\frac{dV_{O_2^-}}{dt} = 128\sqrt{\left(\frac{D_{O_2^-}^3 t}{\pi}\right)}, \quad (19)$$

$$\frac{dV_{HO_2}}{dt} = 128\sqrt{\left(\frac{D_{HO_2}^3 t}{\pi}\right)}, \quad (20)$$

where N_H, N_{OH}, N_e, $N_{H_3O^+}$, N_{OH^-}, N_{H_2}, $N_{H_2O_2}$, $N_{O_2^-}$ and N_{HO_2} are diffusion coefficients from Table I.

At the beginning of this chemical process, only species $H^\bullet$, $OH^\bullet$, e_{aq}^-, H_3O^+, and H_2 are present in the radical cluster. Their initial yield is their initial values for the radical correspondent cluster. The initial volume is the same for all species and depends on the energy transferred to the radical cluster.

3 Using Continuous Petri nets to solve the mathematical model

Continuous Petri nets have been sufficiently described in our previous papers [6][7][8], and here only final results will be presented. The system Visual object net ++ [23] has been used to solve the given system of ordinary differential equations. This visual system allows us to create the mathematical model easily and quickly analyze various situations. The graphical representation of the mathematical simulation model is in Figure 1.

The circles in Figure 1 represent places, and rectangles represent transitions. Each place can be changed via transition connected to it by an arrow. The connection can be performed only between a place and a transition, but never between places or between transitions. The places represent the system's state, and each place is marked by an actual number which determines the value of the monitored parameter.

The places at the top of Figure 1 are not joined with any transitions and represent constants from Table I and Table II (diffusion coefficients and rate coefficients of the chemical reactions).

The values of the cluster volumes are represented by the places on the left of Figure 1 and are changed by the transitions which are joined with them, and are designated as *VH, VOH, Ve, VH3O, VOHM, VH2VH2O2, VOHM,* and *VHO2,* representing the volumes V_H, V_{OH}, V_e, $V_{H_3O^+}$, V_{OH^-}, V_{H_2}, $V_{H_2O_2}$, $V_{O_2^-}$ and V_{HO_2}. At the beginning of the chemical process, all these places have the same value corresponds to the initial volume of the radical cluster, and then the individual volumes containing the corresponding species are increased according to the relevant diffusion coefficients.

The central part of the mathematical simulation model is placed in the middle of Figure 1. The places represent the number of individual species that participate in chemical reactions and are designated as *H, OH, e, H3O, OHM, H2, H2O2, O2M, HO2, O2* and N2O, representing species H, OH, e, H_3O^+, OH^-, H_2, H_2O_2, O_2^-, HO_2, O_2, and N_2O. The value of each place is changed via transitions connected with them. The places and transitions are connected to create a mathematical model that simulates the dynamics of the chemical stage of water radiolysis using the time evolution of the cluster.

The transitions in Figure 1 that cause changes of the chemical species have transition functions in the form:

$$T(H+H) = k_1 \frac{N_H(t)N_H(t)}{V_H(t)}, \quad (21)$$

$$T(H+e) = k_2 \frac{N_H(t)N_e(t)}{V_H(t)}, \quad (22)$$

$$T(e+e) = k_3 \frac{N_e(t)N_e(t)}{V_e(t)}, \quad (23)$$

$$T(OH+e) = k_4 \frac{N_{OH}(t)N_e(t)}{V_e(t)}, \quad (24)$$

$$T(H+OH) = k_5 \frac{N_H(t)N_{OH}(t)}{V_H(t)}, \quad (25)$$

$$T(OH+OH) = k_6 \frac{N_{OH}(t)N_{OH}(t)}{V_{OH}(t)}, \quad (26)$$

$$T(e+H3O) = k_7 \frac{N_e(t)N_{H_3O^+}(t)}{V_{H_3O^+}(t)}, \quad (27)$$

$$T(H+HO2) = k_8 \frac{N_H(t)N_{HO_2}(t)}{V_H(t)}, \quad (28)$$

$$T(OH+HO2) = k_9 \frac{N_{OH}(t)N_{HO_2}(t)}{V_{HO_2}(t)}, \quad (29)$$

$$T(HO2+HO2) = k_{10} \frac{N_{HO_2}(t)N_{HO_2}(t)}{V_{HO_2}(t)}, \quad (30)$$

$$T(H3O+O2M) = k_{11} \frac{N_{H_3O^+}(t)N_{O_2^-}(t)}{V_{H_3O^+}(t)}, \quad (31)$$

$$T(H3O+OHM) = k_{12} \frac{N_{H_3O^+}(t)N_{OH^-}(t)}{V_{H_3O^+}(t)}, \quad (32)$$

$$T(H+H2O2) = k_{13} \frac{N_H(t)N_{H_2O_2}(t)}{V_H(t)}, \quad (33)$$

$$T(e+H2O2) = k_{14} \frac{N_e(t)N_{H_2O_2}(t)}{V_e(t)}, \quad (34)$$

$$T(OH+H2O2) = k_{15} \frac{N_{OH}(t)N_{H_2O_2}(t)}{V_{H_2O_2}(t)}, \quad (35)$$

$$T(OH+H2) = k_{16} \frac{N_{OH}(t)N_{H_2}(t)}{V_{H_2}(t)}, \quad (36)$$

$$T(HO2) = k_{17} N_{(HO_2)}(t), \quad (37)$$

$$T(e+O2) = k_{18} \frac{N_e(t)N_{O_2}(t)}{V_e(t)}, \quad (38)$$

$$T(H+O2) = k_{19} \frac{N_H(t)N_{O_2}(t)}{V_H(t)}. \quad (39)$$

$$T(e+N2O) = k_{20} \frac{N_e(t)N_{N_2O}(t)}{V_e(t)}. \quad (40)$$

The volumes on the left in Figure 1 are changed according to the transition functions:

$$TVH = 128\sqrt{\left(\frac{D_H^3 t}{\pi}\right)}, \quad (41)$$

$$TVOH = 128\sqrt{\left(\frac{D_{OH}^3 t}{\pi}\right)}, \quad (42)$$

$$TVe = 128\sqrt{\left(\frac{D_e^3 t}{\pi}\right)}, \quad (43)$$

$$TVH3O = 128\sqrt{\left(\frac{D_{H_3O^+}^3 t}{\pi}\right)}, \quad (44)$$

$$TVOHM = 128\sqrt{\left(\frac{D_{OH^-}^3 t}{\pi}\right)}, \quad (45)$$

$$TVH2 = 128\sqrt{\left(\frac{D_{H_2}^3 t}{\pi}\right)}, \quad (46)$$

$$TVH2O2 = 128\sqrt{\left(\frac{D_{H_2O_2}^3 t}{\pi}\right)}, \quad (47)$$

$$TVO2M = 128\sqrt{\left(\frac{D_{O_2^-}^3 t}{\pi}\right)}, \quad (48)$$

$$TVHO2 = 128\sqrt{\left(\frac{D_{HO_2}^3 t}{\pi}\right)}, \quad (49)$$

To use the mathematical simulation model presented in Figure 1 for concrete radical cluster, it is necessary to enter the initial values of the individual places, which represent constants from Table I and Table II, the initial number of chemical species, and the initial value of cluster volume.

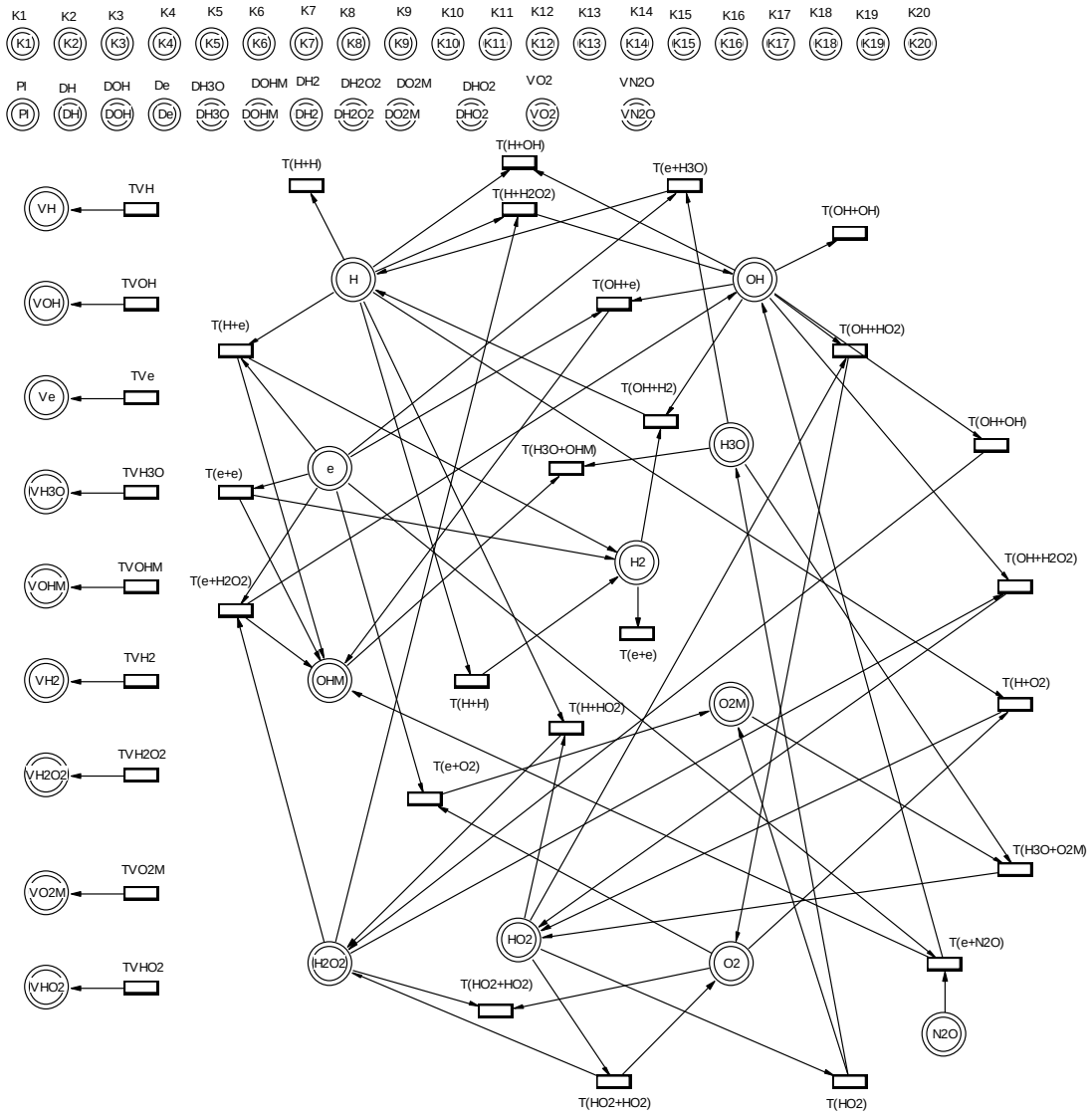

Figure 1. Processes running in radical clusters, represented with the help of Petri nets.

4 Application of the simulation model on the influence of N_2O on the time evolution of cluster radicals

The mathematical simulation model, created with the help of Continuous Petri nets, enables us to simultaneously solve the time evolution of the cluster diffusion with the chemical reactions running inside the cluster. As has been mentioned, the main significance of our mathematical simulation model is the possibility to study not only the influence of various substances on the chemical stage of water radiolysis, but also to study the influence of radioprotective and radiosensitive substances on DNA damage (mainly SSB and DSB formation), which can be very useful not only in radiotherapy, but also in the other fields where living cells are irradiated by ionizing radiation.

The initial size of the radical cluster depends on the amount of transferred energy. Based on our earlier analysis [3][5] of the experimental data presented by Blok and Loman [11], using the optimization procedure, it has been derived that the average initial size of the radical clusters efficient in DNA damage (SSB and DSB formation) corresponds to energy 300 eV and its volume diameter is circa 27 nm.

Immediately at the end of the physicochemical stage (after radical cluster formation), only species $H^{\bullet}$, $OH^{\bullet}$, e_{aq}^{-}, H_3O^{+} and H_2 are present inside the cluster. Their initial numbers N_H, N_{OH},

N_e, $N_{H_3O^+}$, and N_{H_2} can be characterized by radical yield values G^0 under anoxic conditions [14][18][19][20][22]. For transferred energy 300 *eV* [8] it will be put at the time *t = 0*

$$N_{H^\bullet} = 1.26,\ N_{OH^\bullet} = 16.5,\ N_e = 14.34,\ N_{H_3O^+} = 14.34,\ N_{H_2} = 0.45,$$

while the initial numbers of other species will be equal to zero.

The values of diffusion coefficients D_H, D_{OH}, D_e, $D_{H_3O^+}$, D_{OH^-}, D_{H_2}, $D_{H_2O_2}$, $D_{O_2^-}$, D_{HO_2} and of rate constants $k_1 - k_{20}$ are presented in Table I and Table II and are taken from the literature.

A good agreement with experimental data has been achieved to verify our mathematical simulation model under the initial conditions introduced above (cluster diameter 27 nm and energy 300 eV and others) (see Table III).

Table 3. Comparison of the calculated value with experimental results

Substance		Initial yield (G^0)	Experimental yield (G)	Petri nets (G)
1.	$H^\bullet$	0.42	0.62	0.620
2.	$OH^\bullet$	5.5	2.8	2.804
3.	e_{aq}^-	4.78	2.8	2.808
4.	H_3O^+	4.78	2.8	2.802
5.	H_2	0.15	0.47	0.473
6.	H_2O_2	0	0.73	0.733

To study the influence of N_2O on the chemical stage of water radiolysis, and mainly the influence of N_2O on the radiobiological mechanism, the analysis of the time evolution of the radical cluster is instrumental because the prominent role is played by the concentration of radicals at the moment of DNA collision with the radical cluster. The concentration of radicals depends on the distance of DNA molecule from the cluster when radicals begin diffuse into surroundings, and their concentration decreases. The near is DNA to radical cluster, the higher probability of DNA damage is. The presence of N_2O during irradiation increases the concentration of *OH* radicals. Therefore, the analyses of the dependences of *OH* radical concentration on the concentration of N_2O are fundamental. As we will see in the following analyses, a higher concentration of N_2O results in a higher concentration of *OH* radicals and results in a more significant damage of DNA molecules.

In the following part, we will show the time dependencies of individual radical concentrations under various N_2O concentrations, which is very important to analyze the effect of ionizing radiation on living cells. All analyses will be done for cluster diameter 27 nm and energy 300 eV.

In Figure 2, we will start with the time-dependent radical concentrations in saturated O_2 solution without the presence of N_2O.

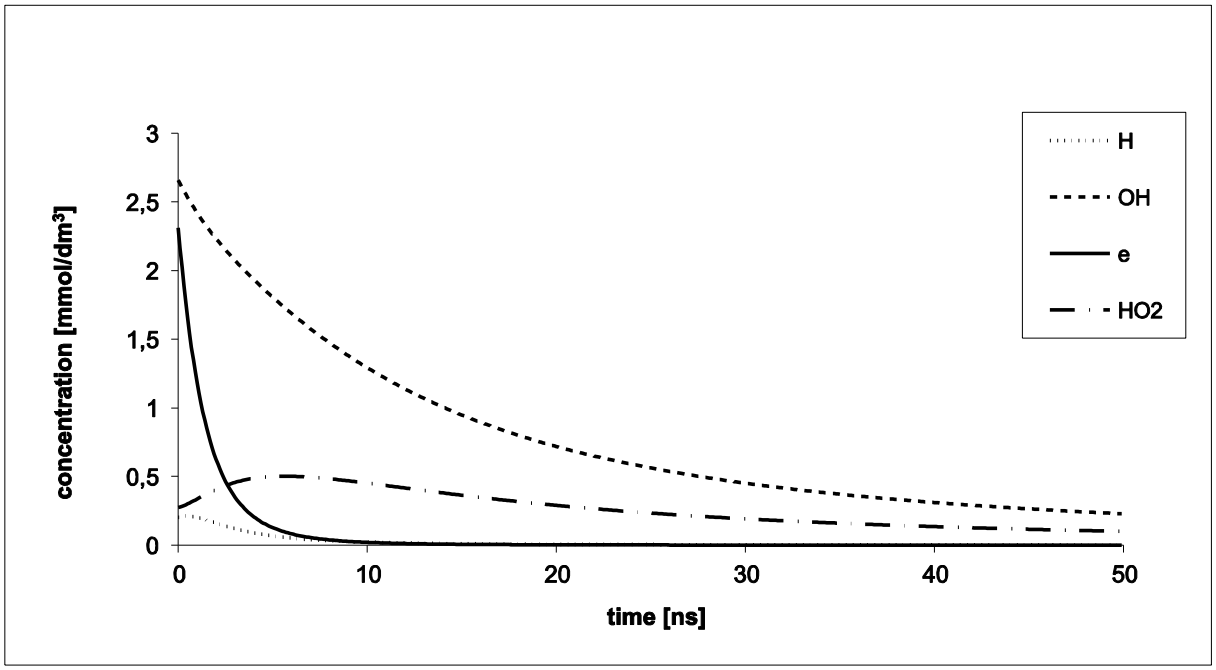

Figure 2. Concentrations depending on the time in saturated O_2 solution without the presence of N_2O.

As shown in Figure 2, the concentration of *OH* radicals is higher than that of other radicals and decreases slower. As a result, *OH* radicals have the most excellent effect on DNA damage, according to generally accepted opinion. The concentration of *H* radicals is deficient and can hardly cause DNA damage. At time *t = 0*, the concentration of hydrated electrons e_{aq}^{-} is nearly as high as the concentration of *OH* radicals but immediately drops sharply with time and also can hardly cause damage to DNA molecules.

At the beginning of the chemical stage, the concentration of HO_2 radicals increases according to reaction 19 (see Table II), and then their concentration decreases by the chemical reactions with other species and their diffusion into surroundings. Nevertheless, their concentration is much lower than the concentration of *OH* radicals, and therefore HO_2 radicals have a much smaller radiobiological effect than *OH* radicals.

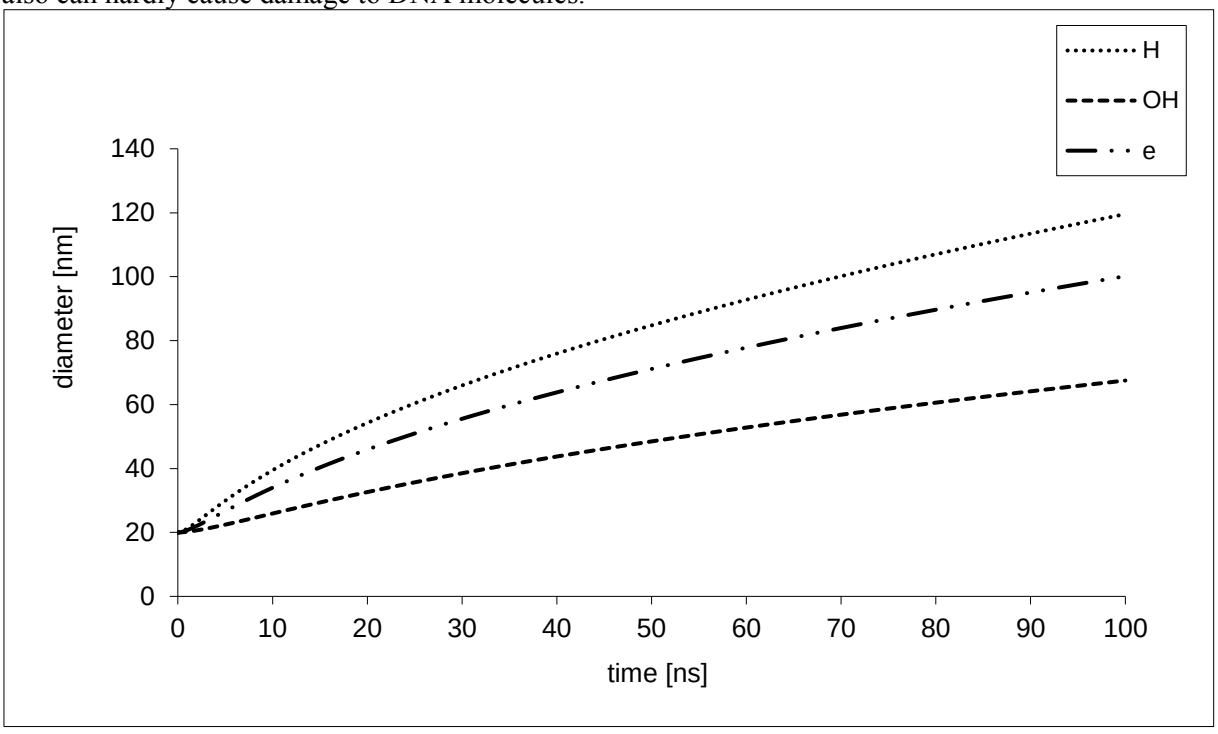

Figure 3. Time dependence of cluster diameters for radicals H, OH, and hydrated electrons e_{aq}^{-}.

In Figure 3, one can see the time changes of cluster diameters for radicals *H*, *OH,* and hydrated electrons e_{aq}^{-}. The time dependence of the HO_2 radicals cluster diameter has been omitted since that *OH,* and HO_2 radicals have similar time dependence because they have nearly the same diffusion coefficients (D_{OH} = 2.2 and D_{HO_2} = 2.3). The diameter of the *OH* radicals cluster increases slower than the cluster diameter of other radicals, and its result is such that a decrease of concentration levels of *OH* radicals is also slowed down.

Comparing Figures 2 and 3, it is possible to find out radical concentration and corresponding cluster size at any time. Only radicals that have sufficient concentration can cause damage to the DNA molecule. We can estimate the distance from the cluster center to the DNA molecule when the concentration of radicals is still sufficient to cause damage to the DNA molecule. It is a fact that the smaller the cluster, the higher the concentration of radicals and vice versa.

Figure 2 shows the time-dependent radical concentrations in saturated O_2 solution without the presence of N_2O. In the following figures, the time-dependent radical concentrations at different N_2O concentrations will be presented. Comparing Figures 2, 4, – 7, one can see that N_2O influences the *OH* concentration the most. The higher the N_2O concentration, the higher *OH* concentration (see Figures 2, 4 – 7, and 9). In a saturated N_2O solution, the concentration of the *OH* radicals is nearly twice as high as in the solution without N_2O (see Figures 2 and 7). As can be predicted from the previous statements, a higher concentration of *OH* radicals should cause a larger number of SSB and DSB on a DNA molecule.

To validate this fact, we can use experimental data presented by Blok and Loman [11], and used in our previous paper [3]. For example, from experimental data in Figure 1 and Table III [3], one can find out that without N_2O, the number of DSB is 0.041 per DNA molecule, and at saturated N_2O solution, the number of DSB is 0.06 per DNA molecule which is nearly twice. Thus, the experimental data are in good agreement with the results obtained using our simulation model.

With increasing N_2O concentration, the concentration of hydrated electrons e_{aq}^{-} slightly decreases (see Figures 2, 4 – 7, and 10), which means that hydrated electrons e_{aq}^{-} can hardly cause DNA damage.

The same applies to radicals *H*, the concentration is minimal from the beginning (see Figures 2, 4 – 7, and 8), and they can hardly cause DNA damage.

The concentration of HO_2 radicals also decreases with the increasing concentration of N_2O (see Figures 2, 4 – 7, and 11) and is much lower than the concentration of *OH* radicals.

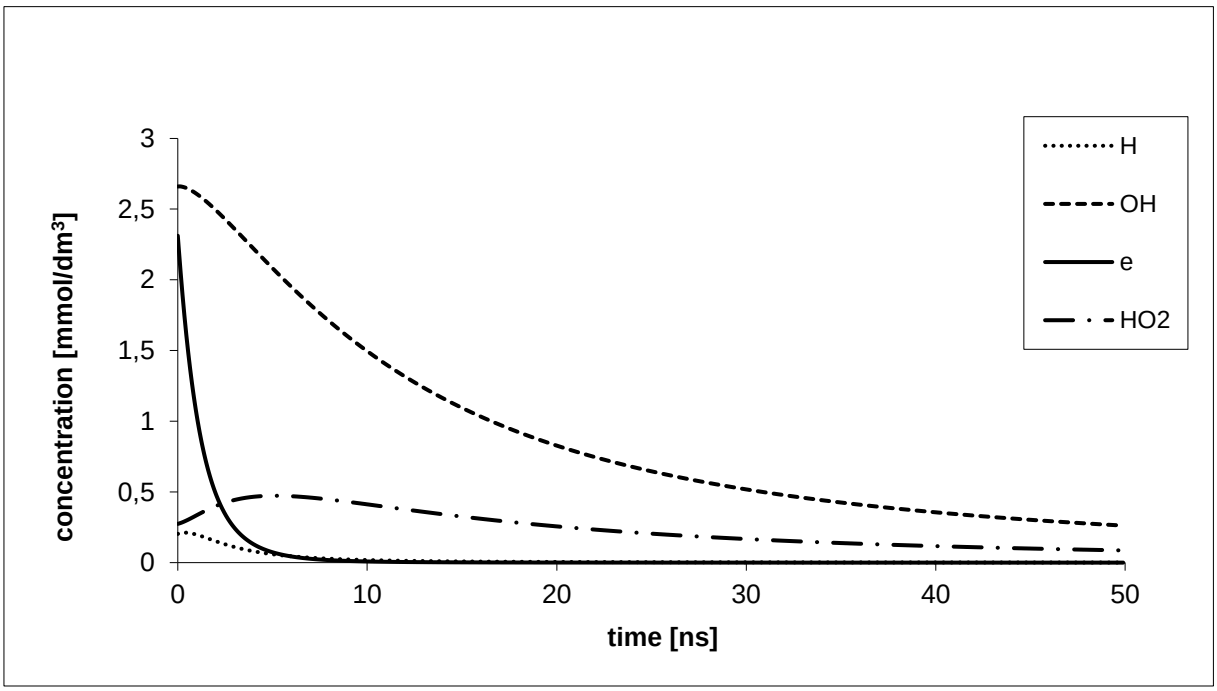

Figure 4. Concentrations depending on the time in saturated O_2 solution at N_2O concentration 1.660 mmol.dm^{-3}.

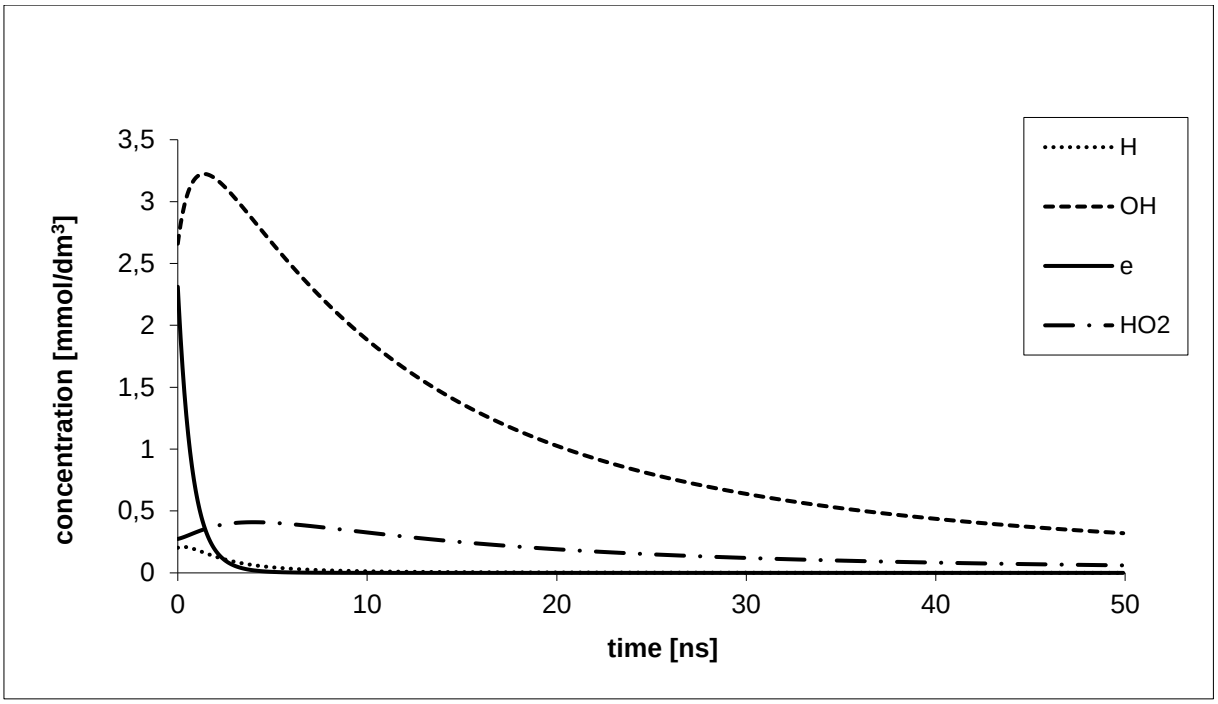

Figure 5. Concentrations depending on the time in saturated O_2 solution at N_2O concentration 8.303 mmol.dm^{-3}.

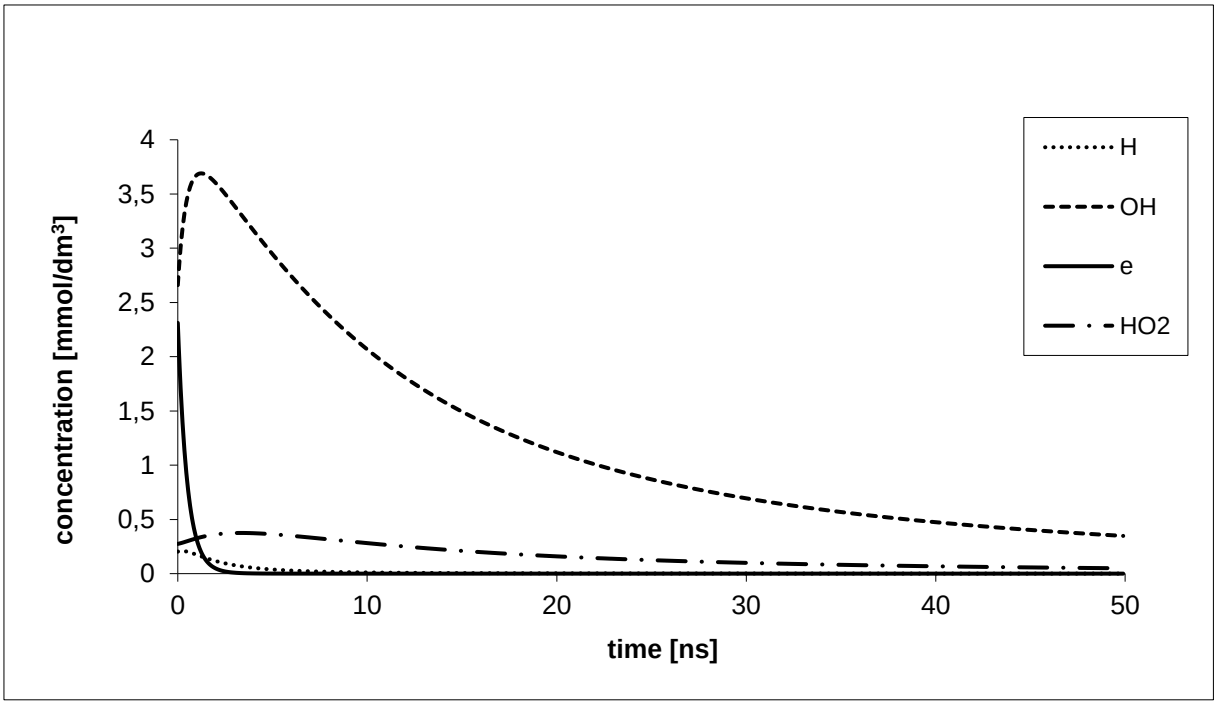

Figure 6. Concentrations depending on the time in saturated O_2 solution at N_2O concentration 16.605 mmol.dm^{-3}.

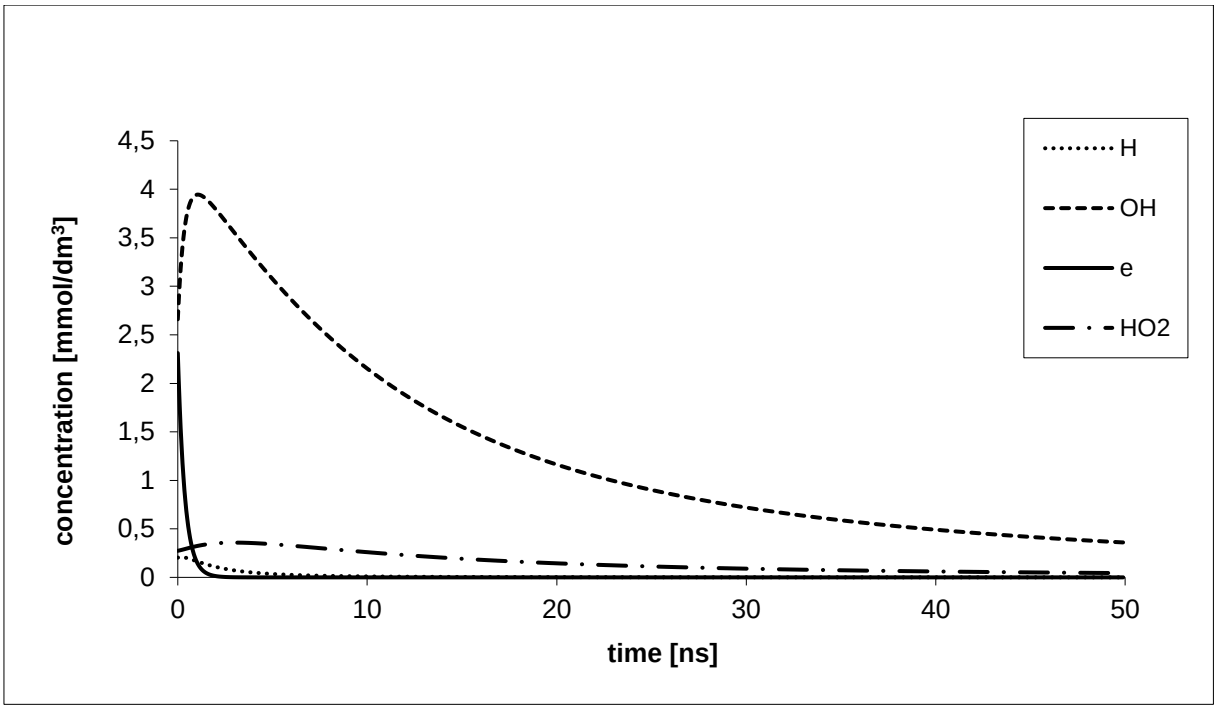

Figure 7. Concentrations depending on the time in saturated O_2 solution at N_2O concentration 24.161 mmol.dm^{-3}.

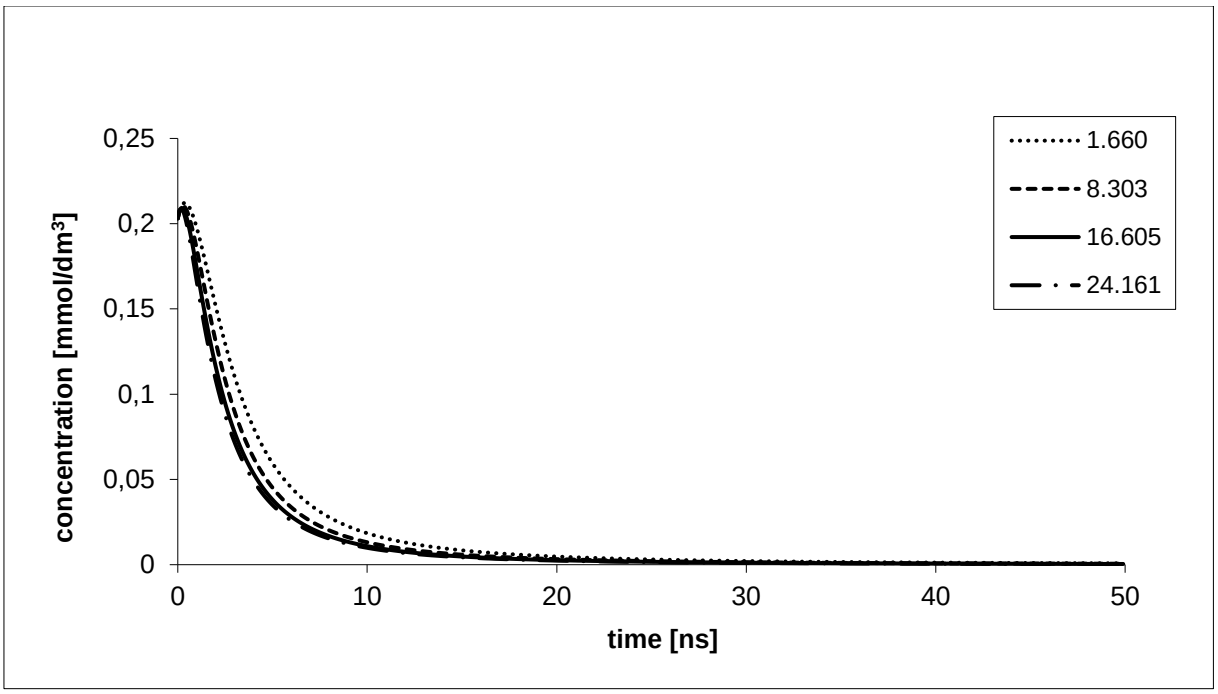

Figure 8. Concentrations depending on the time of H radicals in saturated O_2 solution at various N_2O concentrations [mmol.dm^{-3}].

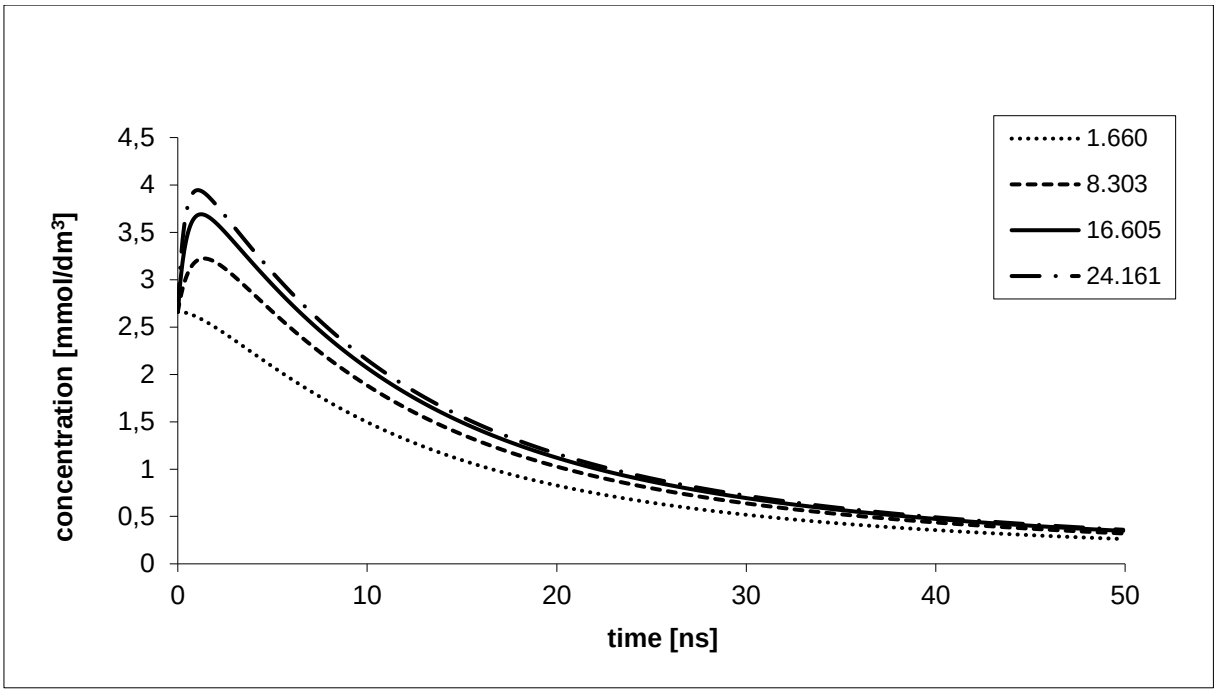

Figure 9. Concentrations depending on the time of OH radicals in saturated O_2 solution at various N_2O concentrations [mmol.dm^{-3}].

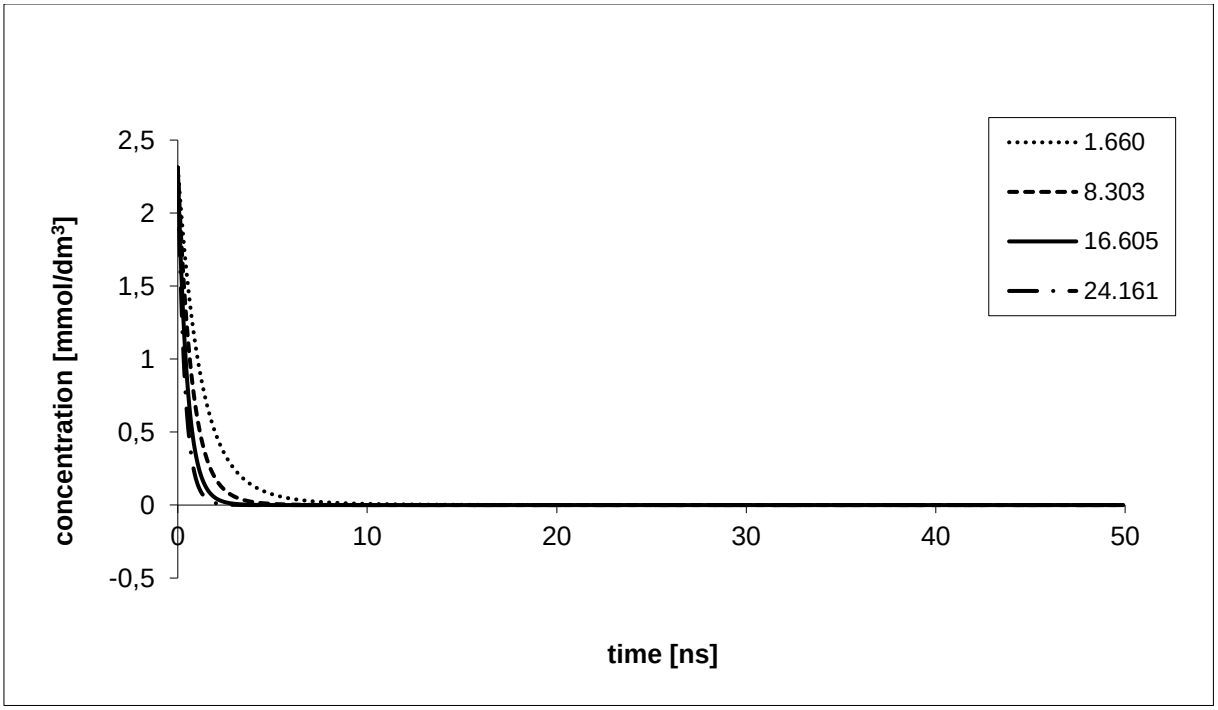

Figure 10. Concentrations depending on the time of hydrated electrons e_{aq}^- in saturated O_2 solution at various N_2O concentrations [mmol.dm^{-3}].

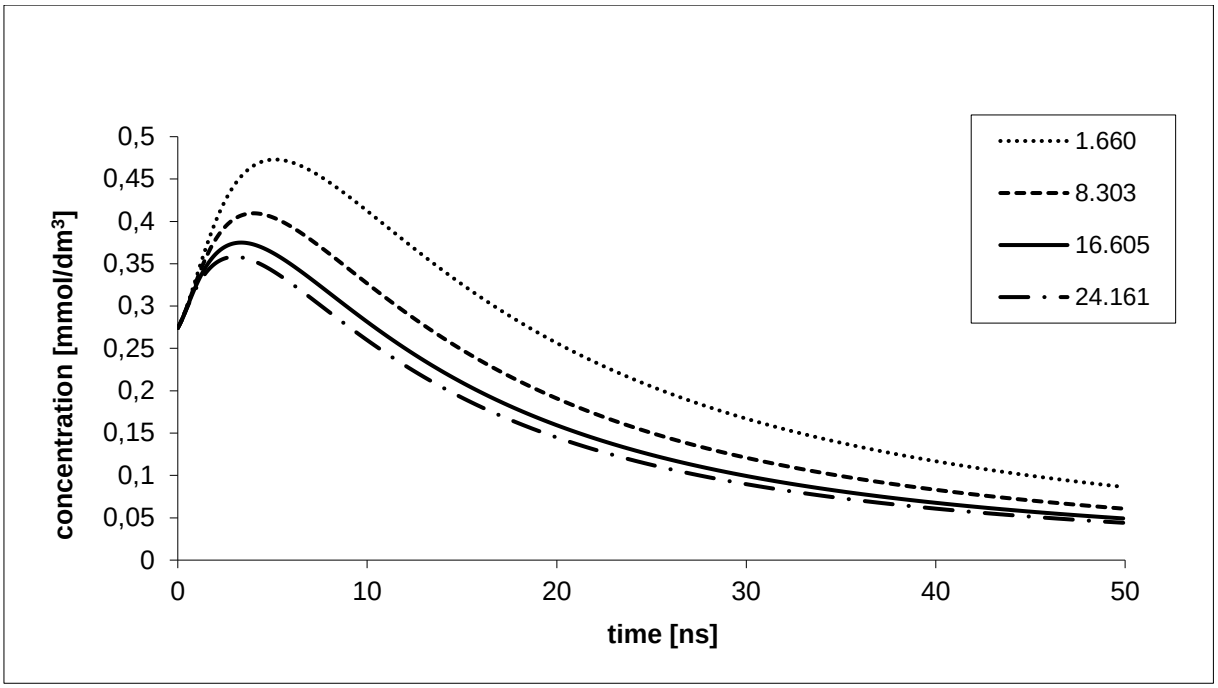

Figure 11. Concentrations depending on the time of HO_2 radicals in saturated O_2 solution at various N_2O concentrations [mmol.dm-3].

The analysis performed based on our simulation model supports our previous results, and it is following the known general opinion that *OH* radicals determine the decisive influence on DNA damage. All these characteristics can be explained based on of reactions considered and summarized in Table II. The chemical reaction of hydrated electrons e_{aq}^{-} with N_2O results in the form of *OH* radicals which significantly contributes to DNA damage. The severe DNA molecule damage is represented by a DSB that is always formed by a pair of radicals from one cluster that meets the corresponding DNA molecule. DSB being formed only when two SSB are formed in different strands.

As the clusters and DNA molecules are distributed randomly in the corresponding space, they meet at different times due to thermal motion and cluster diffusion. The probability of DSB formation can be then given as

$$p_D = \frac{1}{2}\ p_S^2\,, \tag{50}$$

where p_S can be expressed approximately as

$$p_S = \sum_j \int_t \alpha_j\, c_j(t).$$

Parameters α_j represent the efficiency of individual radicals, that take part in forming individual SSB in dependence on the applied dose, and $c_j(t)$ corresponds to the concentration of radicals *j*; DSB is formed only when two SSB are formed in different strands. In the given formula, it has been assumed (for simplicity) that DNA molecules and diffusing clusters have come into mutual contact with the same frequency in different time instants.

The mathematical model of the chemical stage of water radiolysis based on using Continuous Petri nets brings new possibilities in studying regularities in radiobiological processes in dependence on other species present in the corresponding medium.

5 Conclusion

As shown in this work, the presence of N_2O during irradiation of water by ionizing radiation significantly influences radiobiological effect on living cells, mainly if low-LET radiation is used [1][2]. Furthermore, the presence of N_2O molecules in water during irradiation causes the increase of *OH* radical concentration resulting in more significant damage on DNA molecules because *OH* radicals have decisive influence on SSB and DSB formation. This fact can be used in radiotherapy, radiosterilization, food irradiation, and wastewater irradiation.

An indirect effect of ionizing radiation is assumed in our work, where aggressive radicals cause SSB and DSB on DNA molecules. The DNA is damaged during the chemical stage of water radiolysis when energy is transferred to the radical cluster, and the concentration of radicals decreases by their chemical reactions and their diffusion into surroundings. To analyze the effect of ionizing radiation on DNA

damage, the mathematical simulation model is very suitable. However, this mathematical model is very complicated because it includes the diffusion of radicals and their chemical reactions simultaneously. Furthermore, spherical symmetry is assumed for the time evolution of the radical cluster.
Continuous Petri nets were used to solve this complicated mathematical model, because they provide us with the graphical tools to create the mathematical model easily. Creating the mathematical simulation model with the help of Continuous Petri nets is much faster than by classical programming. We are able to perform a great deal of analysis of the studied system and quickly adapt the model to analyze another similar system. Especially research into the influence of radioprotective and radiosensitive substances on the irradiation of living cells with ionizing radiation using mathematical simulation models is very vital.
In our further research, the damage of living cells by ionizing radiation will be simulated with the help of Colored Petri nets because they provide us with better tools for creating a simulation model and its analysis. We will aim to simulate the physical, chemical, and biological stages of the radiobiological mechanism together with reparation processes in a cell.

Acknowledgment

This work was supported by the Faculty of science, J. E. Purkinje University in Usti nad Labem, Czech Republic. English language correction was performed by Saliha Afzaal.

References:

[1] Alizadeh E, Cloutier P, Hunting D, Sanche L., "Soft X-ray and Low Energy Electron Induced Damage to DNA under N2 and O2 Atmospheres", J. Phys. Chem. B 2011; 115:4523–4531. DOI:10.1021/jp200947g

[2] Alizadeh E, Sanche L., "Induction of strand breaks in DNA films by low energy electrons and soft X-ray under nitrous oxide atmosphere", Radiation Physics and Chemistry 2012; 81:33-39. DOI:10.1016/j.radphyschem.2011.09.004

[3] Barilla J, Lokajíček M. "The role of Oxygen in DNA Damage by Ionizing Particles", Journal of Theoretical Biology 2000; 207:405-414. DOI:10.1006/jtbi.2000.2188

[4] Barilla J, Lokajíček M, Pisaková H, et al., "Simulation of the chemical phase in water radiolysis with the help of Petri nets", Curr Opin Biotechnol 2011; 22: S58–S59. DOI:10.1016/j.copbio.2011.05.162

[5] Barilla J, Lokajíček M, Pisaková H, et al., "Analytical model of chemical phase and formation of DSB in chromosomes by ionizing radiation", Australasian Physical & Engineering Sciences in Medicine 2013; 36(1):11-17 DOI:10.1007/s13246-012-0179-4

[6] Barilla J, Lokajíček M, Pisaková H, et al., "Simulation of the chemical stage in water radiolysis with the help of Continuous Petri nets", Radiation Physics and Chemistry 2014; 97:262-269, DOI:10.1016/j.radphyschem.2013.12.019

[7] Barilla J, Lokajicek M, Pisaková H, et al., "Applying Petri nets to modeling the chemical stage of radiobiological mechanism", Physics and Chemistry of Solids 2015; 78:127–136, DOI:10.1016/j.jpcs.2014.11.016

[8] Barilla J., Lokajíček, M., Pisakova, H., Simr, P., "Influence of oxygen on the chemical stage of radiobiological mechanism", Radiation Physics and Chemistry 2016; 124, 116-123. DOI:10.1016/j.radphyschem.2016.01.035
Barilla J., Lokajíček M., Pisakova H., Simr, P., "Using Petri Nets to Model the Chemical Stages of the Radiobiological Mechanism", New York: Nova Science Publishers, 2017; ISBN 978-1-53612-896-3.

[9] Beuve M, Colliaux A, Dabli D, et al., "Statistical effects of dose deposition in track-structure modelling of radiobiology efficiency", Nuclear Instruments and Methods in Physics Research Section B: Beam Interactions with Materials and Atoms 2009; 267:983-988. DOI:10.1016/j.nimb.2009.02.016

[10] Blok J, Loman H., "The effects of γ - radiation in DNA", Curr Top Radiat Res Q. 1973; 9:165-245.

[11] Buxton GV, Swiatla-Wojcik D., "Modeling of Radiation Spur Processes in Water at Temperatures up to 300 C", J. Phys. Chem. 1995; 99:11464–11471. DOI:10.1021/j100029a026

[12] Buxton GV, "High Temperature Water Radiolysis", Radiation Chemistry 2001; 145-162, ed. Jonah, C. D. and Rao, B. S. M. Elsevier, Amsterdam. DOI:10.1016/S0167-6881(01)80009-4

[13] Buxton GV, "The radiation chemistry of liquid water : Principles and applications, in Charged particle and photon interactions with Matter - Chemical, Physicochemical and Biological Consequences with Applications.", 2004; 331-363, ed. Mozumder, A. and Hatano, Y. New York, Marcel Dekker.

[14] Chatterjee A, Maggie J, Dex S., "The Role of Homogeneous Reaction in the Radiolysis of Water", Radiation Research 1983; 96:1-19.

[15] David R, Alia H, "Discrete Continuous and Hybrid Petri nets", Springer-Verlag 2005. DOI:10.1007/b138130

[16] Gu T, Dong R. "A novel continuous model to approximate time Petri nets: Modelling and analysis", Int. J. Appl. Math. Comput. Sci. 2005; 15:141–150.

[17] Hart EJ, Platzman RL, "Radiation Chemistry", Academic Press: New York 1961; 93-257, ed. Errera, M. and Forssberg.

[18] Hervé du Penhoat MA, Goulet T, Frongillo Y, et al., "Radiolysis of Liquid Water at Temperatures up to 300oC: Monte Carlo Simulation Study", J. Phys. Chem. 2000; 41:11757–11770. DOI:10.1021/jp001662d

[19] LaVerne JA, Pimblott SM, "Scavenger and Time Dependences of Radicals and Molecular Products in the Electron Radiolysis of Water", J. Phys. Chem 1991; 95:3196–3206. DOI:10.1021/j100161a044

[20] Mozumder A, Magee JL., "Model of Tracks of Ionizing Radiations of Radical Reaction Mechanisms", Radiation Research 1966; 28:203–214.

[21] Pimblott SM, Mozumder A., "Modeling of Physicochemical and Chemical Processes in the Interactions of Fast Charged Particles with Matter", Charged Particle and Photon Interactions with Matter; Marcel Dekker: New York 2003; 75-103, ed. Mozumder, A. and Hatano, Y. DOI:10.1201/9780203913284.ch4

[22] Rainer D., "Visual Object Net++", Available from: http://www.techfak.uni-bielefeld.de/mchen/ BioPNML/Intro/VON.html. 2008.

[23] Silva M, Recalde L., "On fluidification of Petri net models: from discrete to hybrid and continuous models", Annual Reviews in Control 2004; 28:253–266. DOI:10.1016/j.arcontrol.2004.05.002

[24] Silva M, Julvez J, Mahulea, C., et al., "On fluidization of discrete event models: observation and control of continuous Petri nets", Discrete Event Dynamic Systems 2011; 21:4:427-497. DOI:10.1007/s10626-011-0116-9

[25] Uehara S, Nikjoo H., "Monte Carlo simulation of water radiolysis for low-energy charged particles", Journal of Radiation Research 2006; 47:69–81. DOI:10.1269/jrr.47.69

[26] Watanabe R, Saito K., "Monte Carlo simulation of water radiolysis in oxygenated condition for monoenergetic electrons from 100 eV to 1 MeV", Radiation Physics and Chemistry 2001; 62:217-228. DOI:10.1016/S0969-806X(01)00195-5